NASA Technical Memorandum 106072
ICOMP–93–07; CMOTT–93–02

A Multiple-Scale Model for Compressible Turbulent Flows

William W. Liou and Tsan-Hsing-Shih
Institute for Computational Mechanics in Propulsion and Center for Modeling of Turbulence and Transition
Lewis Research Center
Cleveland, Ohio

March 1993

NASA

A Multiple-Scale Model for Compressible Turbulent Flows

William W. Liou and Tsan-Hsing Shih
Institute for Computational Mechanics in Propulsion
and Center for Modeling of Turbulence and Transition
Lewis Research Center
Cleveland, Ohio 44135

ABSTRACT

A multiple-scale model for compressible turbulent flows is proposed in this paper. It is assumed that turbulent eddy shocklets are formed primarily by the "collisions" of large energetic eddies. The extra straining of the large eddy, due to their interactions with shocklets, enhances the energy cascade to smaller eddies. Model transport equations are developed for the turbulent kinetic energies and the energy transfer rates of the different scale. The turbulent eddy viscosity is determined by the total turbulent kinetic energy and the rate of energy transfer from the large scale to the small scale, which is different from the energy dissipation rate. The model coefficients in the modeled turbulent transport equations depend on the ratio of the turbulent kinetic energy of the large scale to that of the small scale, which renders the model more adaptive to the characteristics of individual flow. The model is tested against compressible free shear layers. The results agree satisfactorily with measurements.

1. INTRODUCTION

Turbulent fluctuations generally cover a broad spectrum of length scales and time scales. Turbulence in the different part of the spectrum reacts differently to changes in the environment. The production of the turbulent kinetic energy due to the deformation of the mean flow is governed by the low wavenumber, or large-scale, fluctuations. Energy cascades to smaller eddies through the vortex stretching mechanism. The dissipation of turbulent kinetic energy is mostly associated with the high wavenumber, or small-scale, fluctuations. Launder and Schiestel[1] and Hanjalic *et al.*[2] (denoted by HLS hereafter) first proposed to use the concept of multiple-time-scale in turbulence model development. The HLS model was devised to characterize the rate of progress of different turbulent interactions and spectral non-equilibrium. The derivation of the model equations was based on a rational extension of single-scale models. They successfully predicted several thin shear flows and flows with large pressure variation. Using the same rational, Kim and Chen[3] (denoted by KC hereafter) developed another multiple-time-scale model. In this model, the source terms in the modeled transport equations for the energy transfer rate and the energy dissipation rate were derived from dimensional analyses. This model has been applied successfully to several different cases[4,5]. For compressible turbulent flows, the energy cascade scenario can play a more significant role than it does in incompressible turbulence.

Compressible turbulence modeling is an essential element of many problems of practical interest, such as external aerodynamic calculations, the design of engine component and jet noise reduction. Initially, based on Morkovin's hypothesis[6], models developed for incompressible flows were applied in compressible turbulent flows calculations. This practice was fairly successful in the prediction of bounded shear layers. The same approach, however, failed to predict adequately the reduced growth rate of compressible free shear layers, which was observed in experiments. Oh[7], Rubesin[8] and VanDromme[9], among others, added compressibility corrections to baseline incompressible models. The corrections were mostly deduced from the assumption that the thermodynamic properties of turbulent fluctuations were related according to certain thermodynamic processes such as the isentropic and the isothermal processes. Models with the various modifications have achieved limited success in compressible turbulent flow predictions. It shows, however, that there are physical characteristics of compressible turbulent flows that are not properly accounted for by most of the models.

Liou and Shih[10] performed a preliminary analysis on the equation for the solenoidal part of the dissipation rate for compressible turbulence. They suggested that the thermodynamic properties of the flow system may be important in the transport of the solenoidal dissipation. Numerical simulations of two-dimensional

(2D) and three-dimensional (3D) compressible turbulence also indicated a similar trend. Passot and Pouquet[11] performed a direct numerical simulation (DNS) of 2D decaying turbulence with the initial *rms* turbulent Mach number up to 2. They showed that, for cases with high levels of the initial turbulent Mach number, concentrated regions of large density gradient are formed intermittently in space and time. Regions of large gradients of turbulent quantities similar to those described in Passot and Pouquet[11] were also observed in a DNS of 3D decaying compressible turbulence[12] and of compressible homogeneous turbulence[13]. These shocklet structures interact rather strongly with the turbulence that provide the favorable environment for the formation of shocklets. It was also shown[11,12] that this interaction caused the raising of the high wavenumber end of the turbulent energy spectrum. Similar phenomena have also been observed in a DNS study of turbulence passing through a shock wave[14]. Therefore, it may be argued that the locally non-equilibrium spectrum is characteristic of compressible turbulence and must be considered in model development.

Another distinguishing feature of compressible turbulence is the energy exchange mechanism between the turbulent kinetic energy and the thermal energy through the action of pressure. In the compressible turbulent kinetic energy equation, pressure-dilatation terms appear explicitly. On the other hand, these pressure-dilatation terms have no effect on the evolution of total turbulent kinetic energy in incompressible turbulence. Kida and Orszag[15] investigated the role that the pressure work played in coupling the turbulent kinetic energy and the internal energy. They found that the coupling effects were intensified with increasing density fluctuations. The magnitude and the direction of the energy exchange were found to be dependent on the flow parameters, such as the Reynolds number and the Mach number. Passot and Pouquet[11] also suggested that the plateaux in the time-evolution of turbulence Mach number seen in their simulations reflected the replenishment of the turbulent kinetic energy at the expense of the internal energy. These observations evidently suggest that the pressure-dilatation terms are important in compressible turbulent flows and have to be modeled.

With the observations from the numerical experiments described above, it seems plausible to us that the formation of shocklet structures and the energy exchange between the turbulent kinetic energy and the thermal energy are two important mechanisms that are associated with compressibility effects. Consequently, they should both be taken into account in the development of models for compressible turbulent flows. Recently, a rather new interpretation of the dilatation dissipation was proposed by Sarkar *et al.*[16] and Zeman[17]. They argue that the dilatational part of the dissipation rate contributes significantly to the total dissipation of the turbulent kinetic energy. Sarkar *et al.*[16] performed an asymptotic analysis for the low Mach number Navier-Stokes equations and constructed a dilatation dissipation

model. The model shows that the ratio of the dilatation dissipation to the traditional solenoidal dissipation is proportional to the square of the turbulent Mach number. Zeman's[17] analysis is built upon the existence of eddy shocklets embedded within energetic turbulent eddies. Taulbee and VanOsdol[18] proposed a model for the sum of the dilatation dissipation and the pressure-dilatation terms. The model involves the solution of a transport equation for the density variance. Sarkar *et al.*[19] developed a pressure-dilatation model through scaling arguments and validated the model for homogeneous shear flows and isotropic turbulence. Predictions of compressible free shear layers with these compressibility corrections have shown the observed reduction of growth rates as the convective Mach number increases.

Turbulent dissipation occurs mainly at high-frequency, less energetic, small-scale fluctuations, which are less influenced by the mean flow. The compressible mean flow interacts directly with the large eddies which govern the production of the turbulent kinetic energy and the energy supply to the small-scale eddies. This is especially true for highly dynamically unstable free shear layers which are known to be very susceptible of compressibility effects.

In this paper, a new multiple-scale model is adopted for compressible turbulent flows. The effects of compressibility on the large-scale and the small-scale eddies are considered in a separate manner. The model in its current form is developed in terms of, but not limited to, mass-weighted average quantities. This allows us to simplify the governing equations and facilitate the model development process. In the following, the governing equations for the mean flow are first outlined. The present multiple-scale model is then described. The results of model calculations of compressible free shear layers are presented in the section that follows.

2. ANALYSIS

2.1 Mean flow equations

The flow properties (say, ϕ) are decomposed into two parts: a mean value and a fluctuation with respect to the mean value. That is,

$$\rho = \overline{\rho} + \rho'' \tag{1.a}$$

$$u_i = \widetilde{u}_i + u_i' \tag{1.b}$$

$$p = \overline{p} + p'' \tag{1.c}$$

$$T = \widetilde{T} + T' \tag{1.d}$$

$$H = \widetilde{H} + H' \tag{1.e}$$

$$\mu = \overline{\mu} + \mu'' \tag{1.f}$$

$$\kappa = \overline{\kappa} + \kappa'' \quad , \quad C_p = \overline{C_p} + C_p'' \tag{1.g}$$

where $\rho, u_i, p, T, H, \mu, \kappa$ and C_p denote density, velocity, pressure, temperature, total enthalpy, molecular viscosity, thermal conductivity, and specific heat. To simplify the final form of the governing mean flow equations, it is customary to use both the Reynolds average ($\overline{\phi}$) and the Favre average ($\widetilde{\phi}$) in the decomposition process. The governing equations for the mean flow may be obtained by substitution of flow properties in the form (1) into the Navier-Stokes equations followed by a Reynolds average of the equations. In the present study, the following assumptions have been applied to simplify the equations for the mean flow: (a) the fluctuations of the molecular diffusivities and the thermodynamic coefficients are negligible, i.e., $\mu'' = 0, \kappa'' = 0$, and $C_p'' = 0$, (b) the boundary-layer approximation is applicable to the mean flow with no pressure gradient in the main stream direction. Thus, the governing equations for the mean flow become,

$$\frac{\partial}{\partial x}(\overline{\rho}\widetilde{u}) + \frac{\partial}{\partial y}(\overline{\rho}\widetilde{v}) = 0 \tag{2}$$

$$\overline{\rho}\frac{\overline{\mathrm{D}}\widetilde{u}}{\overline{\mathrm{D}}t} = \frac{\partial}{\partial y}(\overline{\mu}\frac{\partial \widetilde{u}}{\partial y} - \overline{\rho}\widetilde{u'v'}) \tag{3}$$

$$\overline{\rho}\frac{\overline{\mathrm{D}}\widetilde{H}}{\overline{\mathrm{D}}t} = \frac{\partial}{\partial y}[\frac{\overline{\kappa}}{\overline{C}_p}\frac{\partial \widetilde{H}}{\partial y} + (\overline{\mu} - \frac{\overline{\kappa}}{\overline{C}_p})\frac{\partial}{\partial y}(\frac{\widetilde{u^2}}{2}) - \overline{\rho}\widetilde{H'v'}] \tag{4}$$

where $\frac{\overline{\mathrm{D}}}{\overline{\mathrm{D}}t} = \widetilde{u}\frac{\partial}{\partial x} + \widetilde{v}\frac{\partial}{\partial y}$. The first assumption is usually used in the modeling of compressible flows. The type of flow that fits the second approximation includes turbulent thin shear flows, which are commonly used for model development and validation. The multiple-scale model described in this paper provides a closure link between the mean flow field and the turbulent momentum transfer, $-\overline{\rho}\widetilde{u'v'}$, via turbulent eddy viscosity. A constant turbulent Prandtl number is used in the modeling of $-\overline{\rho}\widetilde{H'v'}$. This model is described in the next section.

2.2 The multiple-scale model

In compressible flows, regions of significant gradients of turbulent quantities may exist. As the compressibility effect increases, turbulent eddy shocklets are likely to form. The intermittent eddy shocklets are formed by the "collision" of large, energetic eddies. The small eddies contain much less energy and are less efficient in the formation of eddy shocklet structures when they collide with other eddies. Thus, the eddy shocklets scale with the energy containing eddies and have more direct influence on the evolution of the large eddies than on the smaller eddies.

The large-scale vortical structures are intensified as they pass through the shocklet. This process enhances the vortex stretching mechanism and increases the spectral energy transfer. The passage of the vortical structures through shock waves may also generate small eddies bypassing the usual route of the vortex stretching mechanism that has already been enhanced. These processes may then cause the spectrum to depart locally from equilibrium. Another mechanism that may also contribute to the non-equilibrium spectrum or the creation of vorticity is strongly related to the pressure fluctuation. It has been shown[12,14] that substantial vorticity is created by the baroclinic terms. The creation of vorticity, however, occurs mainly at the shock wave.

A sketch of the turbulent energy spectrum is shown in Figure 1. As was described above, flow compressibility was assumed to have a direct impact on the energy containing turbulent large eddies or the low wavenumber fluctuations. The turbulent kinetic energy associated with this region is denoted by $\widetilde{k_p}$. The large eddies respond more readily to the deformation of the compressible mean flow. The straining of the large eddies due to the compressibility effects increases the spectral energy transfer, $\widetilde{\epsilon_p}$, to the small scale through the mechanism of vortex stretching. The energy contained in the small scales, $\widetilde{k_t}$, in the high wavenumber part of the energy spectrum is increased as more energy is pumped in from the large eddies. Small-scale eddies may also be generated at the intermittent eddy shocklets. The turbulent kinetic energy is then dissipated at the rate $\widetilde{\epsilon_t}$. To model the compressible turbulent field associated with these two distinct regimes in the kinetic energy spectrum the model transport equations for the turbulent kinetic energy of the large eddy, $\widetilde{k_p}$ and of the small eddy, $\widetilde{k_t}$, the rate of energy transfer from the large eddy to the small eddy, $\widetilde{\epsilon_p}$, and the rate of energy dissipation, $\widetilde{\epsilon_t}$, are solved.

The modeled transport equations for $\widetilde{k_p}$ and $\widetilde{\epsilon_p}$ are,

$$\overline{\rho}\frac{\overline{\mathrm{D}}\widetilde{k_p}}{\overline{\mathrm{D}}t} = \frac{\partial}{\partial y}[(\overline{\mu}+\frac{\mu_T}{\sigma_{\widetilde{k_p}}})\frac{\partial \widetilde{k_p}}{\partial y}] \; + \; \mu_T(\frac{\partial \widetilde{u}}{\partial y})^2 \; - \; \overline{\rho}\widetilde{\epsilon_p} \; + \; \mathbf{fc_1} \tag{5}$$

$$\overline{\rho}\frac{\overline{\mathrm{D}}\widetilde{\epsilon_p}}{\overline{\mathrm{D}}t} = \frac{\partial}{\partial y}[(\overline{\mu}+\frac{\mu_T}{\sigma_{\widetilde{\epsilon_p}}})\frac{\partial \widetilde{\epsilon_p}}{\partial y}] + \; Cp_1\frac{\widetilde{\epsilon_p}}{\widetilde{k_p}}\mu_T(\frac{\partial \widetilde{u}}{\partial y})^2 \; - \; Cp_2'\overline{\rho}\frac{\widetilde{\epsilon_p}^2}{\widetilde{k_p}} \; + \; \mathbf{fc_2} \tag{6}$$

The model equations reflect the idea that the rate of change of a turbulent quantity, say $\widetilde{k_p}$, following a fluid element is the sum of the effects of diffusion, source and sink of $\widetilde{k_p}$. $\mathbf{fc_1}$ represents the energy exchange between the turbulent kinetic energy and internal energy due to compressibility. $\mathbf{fc_2}$ denotes the additional spectral energy transfer caused by the compressibility effects. In this study, we have adopted Sarkar *et al.*'s[19] model for the pressure-dilatation terms to model the thermal-turbulent kinetic energy exchange. That is,

$$\mathbf{fc_1} \; = \; -\alpha_2 M_t \mu_T(\frac{\partial \widetilde{u}}{\partial y})^2 \; + \; \alpha_3 \overline{\rho} M_t^2 \widetilde{\epsilon_p} \tag{7}$$

where $\alpha_2 = 0.15, \alpha_3 = 0.2$ and M_t is a turbulent Mach number defined by

$$M_t = \frac{[2(\widetilde{k}_p + \widetilde{k}_t)]^{\frac{1}{2}}}{\widetilde{a}} \tag{8}$$

where $\widetilde{a}$ is the local mean speed of sound. By using a scaling argument, they propose that the pressure-dilatation contributed by the rapid part of the pressure depends on the production while that by the slow part depends on the dissipation. The partially source and partially sink nature of the model conforms to the thermal-kinetic energy exchange hypothesis assumed here.

To model the effects of the increased spectral energy transfer represented by $\mathbf{fc_2}$, a simple model has been constructed through dimensional reasoning. $\mathbf{fc_2}$ represents a functional of the physical variables that may be used to characterized the compressibility related terms in the turbulent kinetic energy equation. That is,

$$\mathbf{fc_2} \equiv \mathbf{fc_2}(\overline{p}, \overline{\rho}, \widetilde{k}_p, \widetilde{\epsilon}_p, \overline{\mu}) \tag{9}$$

By using the Buckingham Π theorem, three nondimensional parameters can be found. They are

$$\Pi_1 = \frac{\overline{p}}{\overline{\rho}\widetilde{k}_p} \approx \frac{1}{\gamma M_t^2}, \qquad \Pi_2 = \frac{\overline{\mu}\widetilde{\epsilon}_p}{\overline{\rho}\widetilde{k}_p^{\,2}} \approx \frac{1}{Re_t}, \qquad \Pi_3 = \frac{\mathbf{fc_2}}{\overline{\rho}\frac{\widetilde{\epsilon}_p^{\,2}}{\widetilde{k}_p}} \tag{10}$$

At high turbulent Reynolds numbers, the dependence of Π_3 on Π_2 may be dismissed[20]. Π_3 may then be expanded in terms of M_t^2 at the incompressible limit. That is,

$$\Pi_3 = b_1 + b_2 M_t^2 + O(M_t^4) \tag{11}$$

A simple expression for $\mathbf{fc_2}$ may be obtained as the high order terms are neglected. The model equations for $\widetilde{k}_p$ and $\widetilde{\epsilon}_p$ in the present model become,

$$\overline{\rho}\frac{\overline{\mathrm{D}}\widetilde{k}_p}{\overline{\mathrm{D}}t} = \frac{\partial}{\partial y}[(\overline{\mu} + \frac{\mu_T}{\sigma_{\widetilde{k}_p}})\frac{\partial \widetilde{k}_p}{\partial y}] + (1 - \alpha_2 M_t)\mu_T(\frac{\partial \widetilde{u}}{\partial y})^2 - (1 - \alpha_3 M_t^2)\overline{\rho}\widetilde{\epsilon}_p \tag{12}$$

$$\overline{\rho}\frac{\overline{\mathrm{D}}\widetilde{\epsilon}_p}{\overline{\mathrm{D}}t} = \frac{\partial}{\partial y}[(\overline{\mu} + \frac{\mu_T}{\sigma_{\widetilde{\epsilon}_p}})\frac{\partial \widetilde{\epsilon}_p}{\partial y}] + Cp_1\frac{\widetilde{\epsilon}_p}{\widetilde{k}_p}\mu_T(\frac{\partial \widetilde{u}}{\partial y})^2 - (Cp_2 - Cp_3 M_t^2)\overline{\rho}\frac{\widetilde{\epsilon}_p^{\,2}}{\widetilde{k}_p} \tag{13}$$

Note that Zeman[17] and Sarkar *et al.*[16] used M_t^2 as a parameter to relate the dilatational dissipation in compressible flows to the solenoidal dissipation.

Since the small scale is affected by compressibility effects mainly through the increased energy transfer from the large scale, $\widetilde{\epsilon_p}$, the modeled transport equations for $\widetilde{k_t}$ and $\widetilde{\epsilon_t}$ take the following forms,

$$\overline{\rho}\frac{\overline{\mathrm{D}}\widetilde{k_t}}{\overline{\mathrm{D}}t} = \frac{\partial}{\partial y}[(\overline{\mu} + \frac{\mu_T}{\sigma_{\widetilde{k_t}}})\frac{\partial \widetilde{k_t}}{\partial y}] + \overline{\rho}\widetilde{\epsilon_p} - \overline{\rho}\widetilde{\epsilon_t} \tag{14}$$

$$\overline{\rho}\frac{\overline{\mathrm{D}}\widetilde{\epsilon_t}}{\overline{\mathrm{D}}t} = \frac{\partial}{\partial y}[(\overline{\mu} + \frac{\mu_T}{\sigma_{\widetilde{\epsilon_t}}})\frac{\partial \widetilde{\epsilon_t}}{\partial y}] + Ct_1\overline{\rho}\frac{\widetilde{\epsilon_t}\widetilde{\epsilon_p}}{\widetilde{k_t}} - Ct_2\overline{\rho}\frac{\widetilde{\epsilon_t}^2}{\widetilde{k_t}} \tag{15}$$

where the rate of energy transfer out of the large scale, $\widetilde{\epsilon_p}$, serves as a source term in the equation for the small-scale turbulent kinetic energy.

The turbulent eddy viscosity can then be expressed as

$$\mu_T \approx \overline{\rho}\, u\, l \approx \overline{\rho}(\widetilde{k_p} + \widetilde{k_t})^{\frac{1}{2}}\frac{(\widetilde{k_p} + \widetilde{k_t})^{\frac{3}{2}}}{\widetilde{\epsilon_p}} \tag{16}$$

where the turbulent velocity scale, u, is estimated by the square-root of the total turbulent kinetic energy. The length scale is expressed[20] in terms of $(\widetilde{k_p} + \widetilde{k_t})^{\frac{3}{2}}/\widetilde{\epsilon_p}$. The Favre-averaged turbulent momentum flux is given by

$$-\overline{\rho}\widetilde{u'v'} = \mu_T\frac{\partial \widetilde{u}}{\partial y} = C_\mu\overline{\rho}\frac{(\widetilde{k_p} + \widetilde{k_t})^2}{\widetilde{\epsilon_p}}\frac{\partial \widetilde{u}}{\partial y} \tag{17}$$

The turbulent heat flux is modeled through μ_T by a constant turbulent Prandtl number, $\sigma_{\widetilde{H}}$. That is,

$$\mu_{\widetilde{H}} = \frac{\mu_T}{\sigma_{\widetilde{H}}} \tag{18}$$

The model coefficients Cp_1, Cp_2, Ct_1, and Ct_2 can be determined by applying the model to simple incompressible flows, including homogeneous and decaying turbulence[21]. The coefficients are,

$$Cp_1 = (1 - \frac{\beta}{\alpha}) + \frac{\beta}{\alpha}Cp_2 \tag{19}$$

$$Cp_2 = \frac{n+1}{n} \tag{20}$$

$$Ct_1 = 1 - \frac{1}{\beta} + \frac{Ct_2}{\beta} \tag{21}$$

$$Ct_2 = \frac{\beta - 1 + Cp_2\beta\frac{\widetilde{k_t}}{\widetilde{k_p}}}{\beta + \beta\frac{\widetilde{k_t}}{\widetilde{k_p}} - 1} \tag{22}$$

where n is the decay rate of grid turbulence. α denotes the ratio of the production rate of the turbulent kinetic energy to the rate of energy transfer from the large scale to the small scale and β denotes the ratio of the rate of energy transfer to the dissipation rate in homogeneous shear flow. The model parameters are summarized in Table 1.

Table 1. Model parameters

C_μ	$\sigma_{\widetilde{k_p}}$	$\sigma_{\widetilde{k_t}}$	$\sigma_{\widetilde{\epsilon_p}}$	$\sigma_{\widetilde{\epsilon_t}}$	n	α	β
0.09	1.0	1.0	1.3	1.3	1.2	2.2	1.05

The validity of the model coefficients was tested against incompressible free-mixing layers, plane jets, and axisymmetric jets. The results were reported in Duncan *et al.*[21]. The details of the derivation of the model coefficients can also be found in Duncan *et al.*[21]. The value of the model coefficient, Cp_3, in the model for the increased energy transfer from the large scale to the small scale will be determined later by calculations. Note that the model coefficients, Ct_1 and Ct_2, are functions of $\widetilde{k_t}/\widetilde{k_p}$. As a result, the model is adaptable to the individual flow conditions and may have a broad range of applicability. The present multiple-scale model was tested in compressible free shear layers of air. The flow geometry is shown in Figure 2. The compressible free shear layer has been known to spread at a slower rate than an equivalent incompressible free shear layer of the same density and velocity ratios. It is generally recognized that the reduced spreading rate is largely due to the effect of compressibility and that the compressible free shear layers are appropriate test cases for compressible turbulence models. The present model has been applied successfully to study compressible plane free shear layers. Some of the results of the calculations are presented in the next section.

3. RESULTS AND DISCUSSIONS

As was noted earlier, the present multiple-scale model, less the compressibility correction terms, has been validated in incompressible turbulent free shear flows using a separate boundary layer code[21]. The model predictions have shown good agreement with measurements. This is true not only for the flow quantity profiles, but also for the growth rate. The results[21] showed that the model predicted correctly the growth rates of both plane jets and axisymmetric jets without using any of the so called "axisymmetric correction" terms. In the present study, the governing equations are solved by using the STAN5 code. The code solves the boundary layer equations by using the Patankar and Spalding[22] procedure. The boundary conditions for the mean turbulent quantities are that the normal gradients are zero

at the boundaries of the computational domain. These zero-gradient boundary conditions have been enforced in all of the calculation performed in this study.

For validation purposes the current multiple-scale model, without including the compressibility effects, is first applied to an incompressible plane free shear layer. The ratio of the speeds of the free stream $r(=\widetilde{u}_2/\widetilde{u}_1)$ is 0.01. Results obtained by using the HLS and the KC multiple-time-scale models, and the standard high Reynolds number $k-\epsilon$ model[23] (denoted by $sk\epsilon$) are also included for comparison. Figure 3 shows the nondimensionalized mean velocity profile, U^*, in a self-similar coordinate, $(y-y_{0.5})/\delta$, where

$$U^* = \frac{(\widetilde{u}-\widetilde{u}_2)}{(\widetilde{u}_1-\widetilde{u}_1)} \tag{23}$$

δ stands for the distance between $y_{0.1}$ and $y_{0.9}$ across the shear layer. $y_{0.1}, y_{0.5}$ and $y_{0.9}$ denote the transverse locations where the values of U^* are 0.1, 0.5, and 0.9, respectively. The model predictions agree well with the experiment. All the calculations were performed with the same initial and boundary conditions. It was assumed that a free shear layer had become self-similar if the profile shapes of the mean velocity and the mean turbulent quantities were independent of the location in the streamwise direction. This criteria of self-similarity was also applied in the calculations of compressible free shear layers in this study. The Reynolds shear stress distributions are shown in Figure 4. The current model predictions agree well with the measurement except at the low speed portion of the layer. The total turbulent kinetic energy profiles are given in Figure 5. Overall, the present model, the HLS model, and the $sk\epsilon$ model predict satisfactorily the profiles of the turbulent kinetic energy and the Reynolds shear stress. However, it was found that the HLS model often produced negative values for the turbulent kinetic energy at the high-speed edge of the layer. This may be the cause for the relatively sharp approach of the local mean velocity toward the free stream velocity in that region. It is also found that the turbulent kinetic energy obtained by using the HLS model oscillates at the outer edges of the shear layer while the flow is developing. Therefore, the HLS model predicts that the flow becomes self-similar farther downstream when compared to the rest of models tested. Similar phenomenon was also observed in Duncan *et al.*[21], where a different boundary layer code was used. They found that the HLS model was relatively more sensitive to the initial conditions compared to the current model, the KC model, and the $sk\epsilon$ model. The oscillatory behavior of the turbulent quantities calculated by using the HLS model becomes more of a problem when the HLS model is extended directly to the calculations of compressible free shear layers.

A possible remedy is to assume the turbulent eddy viscosity is constant at the outer edges[25]. That is, in the region where $U^* > 0.9$, the turbulent eddy

viscosity assumes its value at the location $y = y_{0.9}$ and, similarly, in the region where $U^* < 0.1$, the turbulent eddy viscosity is set equal to its value at $y = y_{0.1}$. This procedure predicted a slight reduction of the growth rate with increasing Mach number. However, it was found that this technique could lead to distorted profiles of the turbulent and mean quantities in the constant eddy viscosity regions and, subsequently, affected the evaluation of the growth rate of a shear layer at high Mach numbers. In the following, the HLS model predictions of compressible free shear layers are not included.

To further verify the implementation of the various models in the code, the growth rate parameter, σ, of free mixing layers for Mach number ranging from one to five were calculated. The results were compared with Launder *et al.*[23], which also used the same $sk\epsilon$ model (denoted by $k\epsilon 1$ in Launder *et al.*[23]). The growth rate parameter was defined as[26],

$$\sigma = \frac{1.855}{\delta'} \tag{24}$$

where $\delta' = \mathrm{d}\delta/\mathrm{d}x$. The results are shown in Figure 6. The values of σ predicted by the current implementation of the $sk\epsilon$ model agree well with those of Launder *et al.*[23]. The predictions obtained by using the current multiple-scale model, less the compressibility correction terms $\mathbf{fc_1}$ and $\mathbf{fc_2}$, follow closely the results of the $sk\epsilon$ model. The growth rate, δ', predicted by both of the models decrease only slightly with increasing Mach numbers. The agreement of the results of the current implementation of the $sk\epsilon$ model and that by Launder *et al.*[23] provides additional support to the results of the present calculations. In the following calculations, the compressibility corrections terms, $\mathbf{fc_1}$ and $\mathbf{fc_2}$, are included. The results are compared with measurements.

Figure 7 shows the calculated variation of the vorticity thickness growth rate of compressible free shear layers, δ'_ω, as a function of a convective Mach number. The compressible growth rate was normalized by the incompressible growth rate (for the same density and velocity ratios), which was obtained by using the following relation[27],

$$\delta'_\omega(M_c = 0, r, s) = C_{\delta_\omega} \frac{(1-r)(1+s^{\frac{1}{2}})}{1+rs^{\frac{1}{2}}} \tag{25}$$

where $s = \overline{\rho}_2/\overline{\rho}_1$ denoted the ratio of the density of the free streams. The value of the constant of proportionality, C_{δ_ω}, was obtained based on present model calculations performed at the limit of $M_c \to 0$. The vorticity thickness, δ_ω, was defined by,

$$\delta_\omega = \frac{\widetilde{u}_1 - \widetilde{u}_2}{(\frac{\mathrm{d}\widetilde{u}}{\mathrm{d}y})_{\mathrm{max.}}} \tag{26}$$

The convective Mach number was defined by the ratio of the average convective velocity of the dominant large-scale structures, relative to the free stream, to the free stream speeds of sound[27]. That is,

$$M_c = \frac{\widetilde{u}_1 - \widetilde{u}_2}{\widetilde{a}_1 + \widetilde{a}_2} \tag{27}$$

The convective Mach number has been shown to be an appropriate parameter to correlate experimental data. In the present study the convective Mach number of the shear layer is increased by increasing the Mach number of the high-speed stream.

Measured data are denoted by open symbols in Figure 7. The current model predictions are denoted by solid circles. The predictions are for conditions in the range, $0.01 < r < 0.36$ and $0.05 < s < 1.0$. The value of Cp_3 is set equal to 3.8. With the inclusion of the compressibility effects, the present compressible multiple-scale model predicts the observed reduction of the vorticity thickness growth rate as the convective Mach number increases. The calculated growth rate curve tends to level off at high convective Mach numbers. According to the definition of the convective Mach number, there exists a maximum convective Mach number for a plane mixing layer of the same fluid with matched total temperature. That is,

$$\lim_{M_f \to \infty} M_c = \frac{1 - r}{\left(\frac{(\gamma-1)(1-r^2)}{2}\right)^{\frac{1}{2}}} \tag{28}$$

where γ denotes the ratio of the specific heats of the fluid. For example, for a value of r=0.1, the limiting convective Mach number for a compressible free shear layer of air is about 2.0.

Figure 7 also shows that, without compressibility correction terms, the normalized growth rates predicted by all of the models tested increase with increasing convective Mach numbers, despite of the fact that their absolute values decrease slightly. Note that the calculated growth rate of the vorticity thickness of a compressible free shear layer is normalized by that of the equivalent incompressible free shear layer of the same velocity and density ratios. According to Eq. (27), for $r = 0.1$, the value of growth rate of the equivalent incompressible shear layer decreases by as much as thirty percent, as the convective Mach number increases from 0 to 1.58. Consequently, the normalized growth rate predictions increase with increasing M_c. It should also be noted that this normalization procedure is in accord with experimental observations.

Also included in Figure 7 is the $sk\epsilon$ model prediction with the Sarkar *et al.*[16] dilatation dissipation model. The results are represented by solid triangles. The dilatation dissipation model can be written as,

$$\widetilde{\epsilon} = \widetilde{\epsilon}_s + \widetilde{\epsilon}_d = (1 + M_t^2)\widetilde{\epsilon}_s \tag{29}$$

where $\widetilde{\epsilon_s}$ and $\widetilde{\epsilon_d}$ denote the solenoidal and dilatation part of the dissipation rate. The model predictions of the growth rate, normalized by the equivalent incompressible values, are higher than the measurements in the high M_c regime. This trend is consistent with the results of Viegas and Rubesin[33], in which the dilatation dissipation model is included in the $sk\epsilon$ calculations of compressible free shear layers.

Since the Reynolds shear stress appears in the mean momentum equations and directly influences the development of the mean flow, it is interesting to see how its peak value varies as a function of M_c. In Figure 8, the peak Reynolds shear stresses predicted by the present compressible multiple-scale model are compared with measured data[34]. The predictions show a decrease of the peak Reynolds shear stresses as the convective Mach number increases. This is consistent with experimental observations. The model also suggests that the peak Reynolds shear stresses are nearly independent of the velocity and density ratios of the free streams. The convective Mach number appears to be an appropriate parameter to correlate the peak Reynolds shear stress of compressible free shear layer. It has been shown[34] that the decreasing trend of the level of the Reynolds shear stress, as the convective Mach number is increased, is due mainly to the decrease of momentum thickness growth rate. Therefore, it is not surprising to see the good correlation of the peak Reynolds shear stresses with the convective Mach number in the present model predictions.

To further validate the present compressible multiple-scale model, the model is applied to compute the compressible free shear layer corresponding to the Case 1 in Samimy and Elliott[29]. In this case, a fully expanded free shear layer of air with $M_c = 0.51$ and $r = 0.36$ is examined. The calculated self-similar mean velocity profile shown in Figure 9 agrees well with the measurement. The predicted and the measured peak Reynolds shear stresses for this case have already been included in Figure 8.

4. SUMMARY

The model for compressible turbulent shear flows proposed here is based on the assumed discrimination of turbulent eddies by compressibility. The large eddies are affected significantly by compressibility. On the other hand, the small eddies are less influenced. It is assumed that, as a direct consequence of compressibility, the process of spectral energy transfer from the large eddies to the small eddies is enhanced and the spectrum is locally non-equilibrium. In the present study, the characteristics of turbulence associated with these two regimes of distinct compressibility effects is modeled by an eddy viscosity model. Together with the proposed compressibility models, the present multiple-scale model performed quite well in the prediction of

compressible free shear layers. This agreement provides further supports to the multiple-scale approach in the modeling of compressible turbulent shear flows.

The present multiple-scale model is being tested for other bounded and unbounded turbulent shear flows, such as boundary layers and jets. Unlike free-mixing layers tested here, the characteristic scales of jet vary as the flow evolves downstream. Therefore, it is possible that the effect of compressibility on turbulence also changes in some fashion. Compressible boundary layers are also challenging cases due to the wall heat transfer constraints.

REFERENCES

[1] B. E. Launder and R. Schiestel, "Sur l'utilisation d'échelles temporelles multiples en modélisation des écouplements turbulents," C. R. Acad. Sci. Ser. A: **286**, 709 (1978).

[2] K. Hanjalic, B. E. Launder and R. Schiestel, "Multiple-time-scale concepts in turbulent transport modeling," **Turbulent Shear Flow 2** (1980).

[3] S. W. Kim and C. P. Chen, "A multiple-time-scale turbulence model based on variable partitioning of turbulent kinetic energy spectrum," NASA CR-179222 (1987).

[4] S. W. Kim, "Calculation of reattching shear layers in divergent channel with a multiple-time-scale turbulence model" NASA TM 102293 (1989).

[5] S. W. Kim, "Numerical investigation of separated transonic turbulent flows with a multiple-time-scale turbulence model," Numerical Heat Transfer **5** (1990).

[6] M. V. Morkovin, "Effects of compressibility on turbulent flows," *The Mechanics of Turbulence*, Favre, A. edt. (Gordon and Breach, New York, 1961).

[7] Y. H. Oh, "Analysis of two-dimensional free turbulent mixing," AIAA paper 74-594.

[8] M. W. Rubesin, "Extra compressibility terms for Favre-averaged two-equation models of inhomogeneous turbulent flows," NASA CR 177556 (1990).

[9] D. D. Vandromme and H. H. Minh, "Solution of the compressible Navier-Stokes equations: Applications to complex turbulent flows," Von Karman Institute Lecture Series on CFD (1983).

[10] W. W. Liou and T. H. Shih, "On the basic equations for the second-order modeling of compressible turbulence," NASA TM 105277 (1991).

[11] T. Passot and A. Pouquet, "Numerical simulation of compressible homogeneous flows in the turbulent regime," J. Fluid Mech. **181**, 441 (1987).

[12] S. Kida and S. A. Orszag, "Energy and spectral dynamics in forced compressible turbulence," J. Sci. Comp. **5**, (1990).

[13] G. A. Blaisdell, N. N. Mansour and W. C. Reynolds, "Numerical simulations of compressible homogeneous turbulence," Rept. TF-50, Dept. of Mechanical Eng., Stanford Univ. (1991).

[14] S. Lee, S. K. Lele and P. Moin, "Direct numerical simulation and analysis of shock turbulence interaction," AIAA paper 91-0523.

[15] S. Kida and S. A. Orszag, "Enstrophy budget in decaying compressible turbulence," J. Sci. Comp. (1991)

[16] S. Sarkar, G. Erlebacher, M. Y. Hussaini and H. O. Kreiss," The analysis and modeling of dilatational terms in compressible turbulence," NASA CR 18195 (1989).

[17] O. Zeman, "Dilatation dissipation: The concept and application in modeling compressible mixing layers," Phys. Fluids **2**, 178 (1990).

[18] D. Taulbee and J. VanOsdol, "Modeling turbulent compressible flows: the mass fluctuating velocity and squared density," AIAA paper 91-0524.

[19] S. Sarkar, G. Erlebacher and M. Y. Hussaini, "Compressible homogeneous shear: simulation and modeling," NASA CR 189611 (1992).

[20] H. Tennekes and J. L. Lumley, *A First Course in Turbulence* (The MIT Press, 1972).

[21] B. S. Duncan, W. W. Liou and T. H. Shih, "A multiple-scale turbulence model for incompressible flow," AIAA paper 93-0086.

[22] S. V. Patankar and D. B. Spalding, *Heat and Mass Transfer in Boundary Layers* (International Textbook Company Ltd., London, 1970).

[23] B. E. Launder, A. Morse, W. Rodi and D. B. Spalding, "Prediction of free shear flows a comparison of the performance of six turbulence models," NASA SP-321, 361 (1972).

[24] R. P. Patel, "An experimental study of a plane mixing layer," AIAA J. **11**, 67 (1973)

[25] G. Fabris, P. T. Harasha and R. B. Edelman, "Multiple-scale turbulence modeling of boundary layer flows for scramjet applications," NASA CR-3433 (1981).

[26] *Proceedings of Conference on Free Turbulent Shear Flows*, Held at NASA Langley Research Center, NASA SP-321 (1972).

[27] D. Papamoschou and A. Roshko, "The compressible turbulent shear layer: an experimental study," J. Fluid Mech. **197**, 453 (1988).

[28] S. G. Goebel and J. C. Dutton, "Experimental study of compressible turbulent mixing layers," AIAA J. **29** (1990).

[29] M. Samimy and G. S. Elliott, "Effects on compressibility on the characteristics of free shear layers," Phys. Fluids **28**, 439 (1990).

[30] G. A. Sullins, "Shear layer mixing tests," NASP CR 1053 (1989)

[31] N. L. Messersmith, S. G. Goebel, W. H. Frantz, E. A. Krammer, J. P. Renie, J. C. Dutton and H. Krier, "Experimental and analytical investigations of supersonic mixing layers," AIAA paper 88-0702.

[32] N. Chinzei, G. Masuya, T. Komuro, A. Murakami and K. Kudou, " Spreading of two-stream supersonic turbulent mixing layers," Phys. Fluids **29**, 1345 (1986).

[33] J. R. Viegas and M. W. Rubesin, "A comparative study of several compressibility corrections to turbulence models applied to high-speed shear layers," AIAA paper 91-1783.

[34] G. S. Elliott and M. Samimy, "Compressibility effects in free shear layers," Phys. Fluids. (1991)

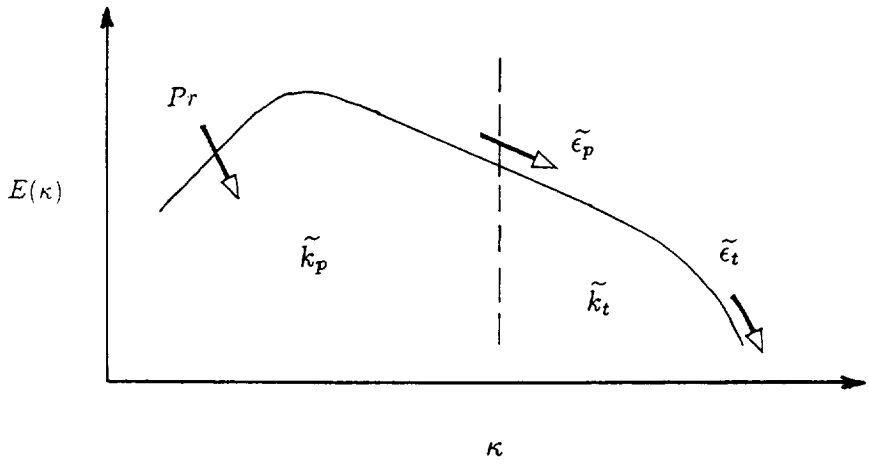

Figure 1. The division of energy spectrum adopted by the present multiple-scale model.

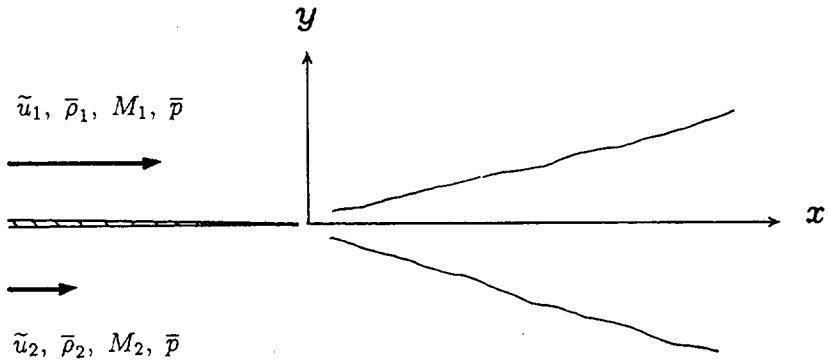

Figure 2. Flow geometry of compressible free shear layers.

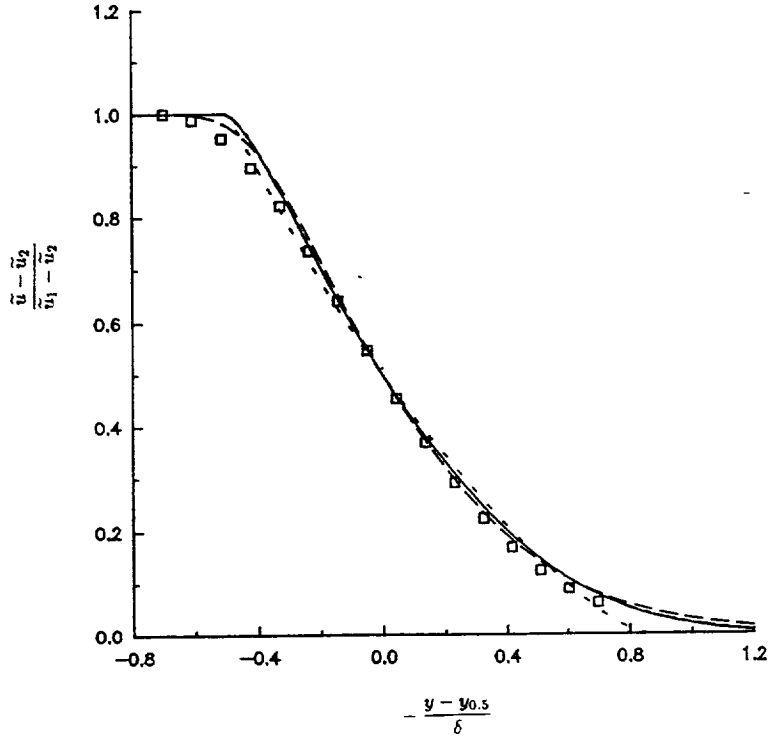

Figure 3. Nondimensional axial mean velocity profiles for incompressible plane mixing layer. ———, present model; - ——, $sk\epsilon$ model; — — , KC model; - - - -, HLS model; □ , Patel[24].

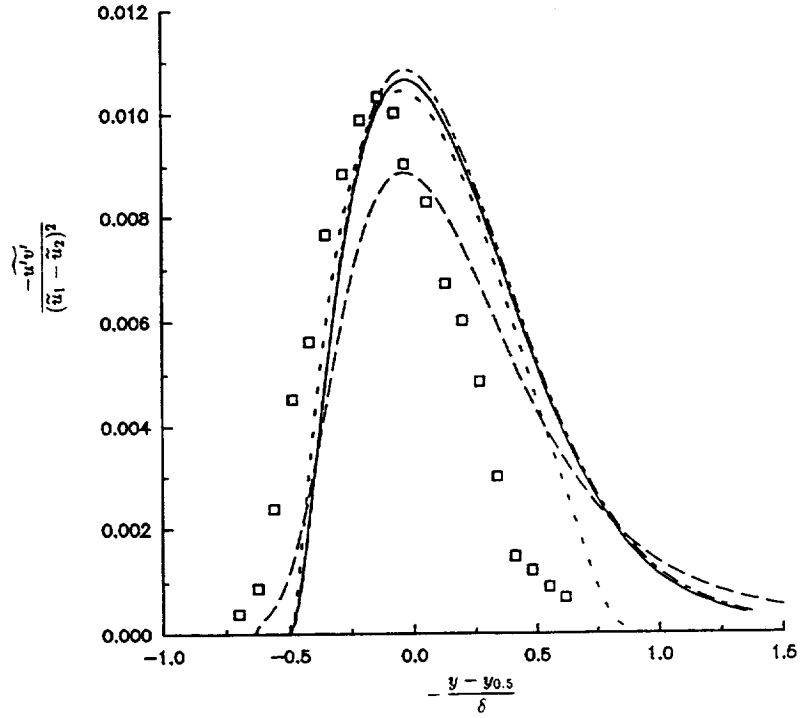

Figure 4. Nondimensional Reynolds shear stress profiles for incompressible plane mixing layer. ———, present model; - ——, $sk\epsilon$ model; — ––, KC model; - - - -, HLS model; □ , Patel[24].

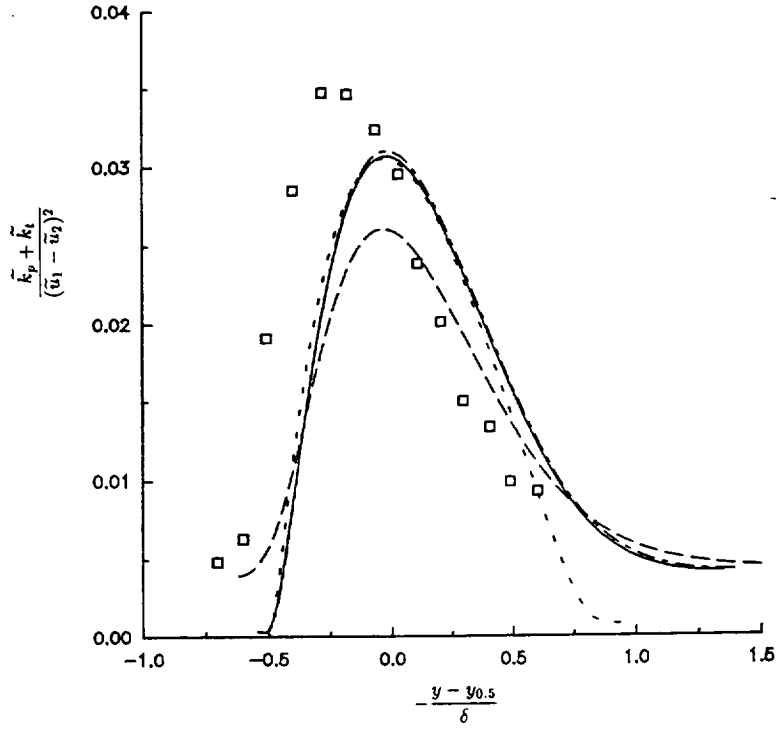

Figure 5. Nondimensional turbulent kinetic energy for incompressible plane mixing layer. ———, present model; - ——, $sk\epsilon$ model, — — , KC model; - - - - , HLS model; □ , Patel[24].

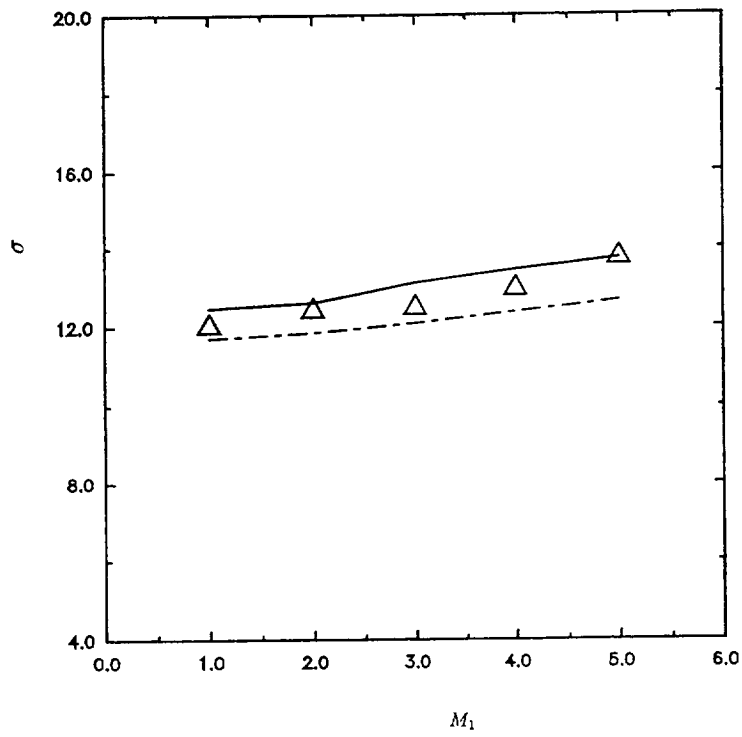

Figure 6. Variation of growth rate parameter with Mach number. ———, present model without compressibility corrections. $sk\epsilon$: - ——, current implementation; △ , Launder *et al.*[23].

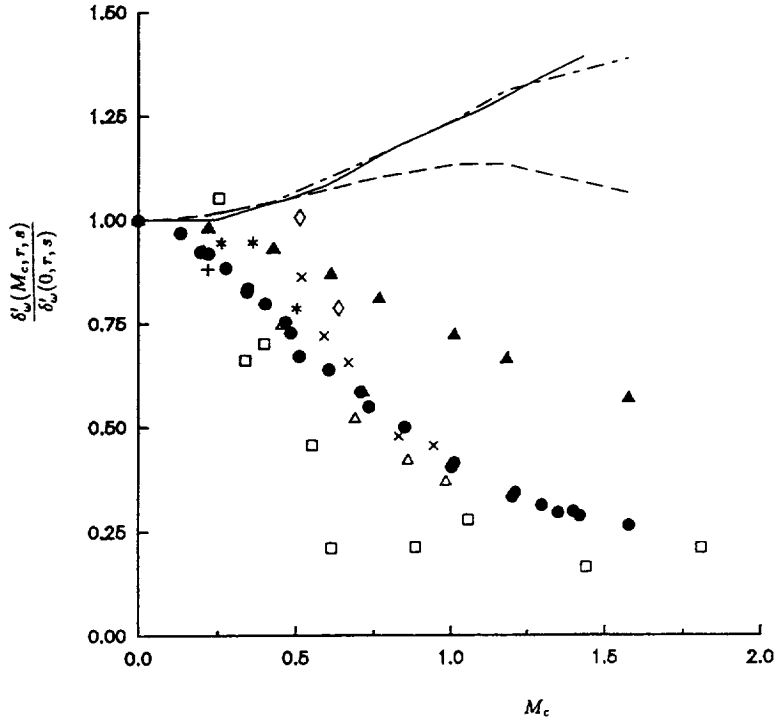

Figure 7. Variation of relative vorticity thickness growth rate with convective Mach number. ●, present model; ———, present model without compressibility corrections; - ——, $sk\epsilon$ model; ▲, $sk\epsilon$ model with Sarkar *et al.*[16] dilatation dissipation model; — — , KC model; □, Papamoschou and Roshko[27]; △, Goebel *et al.*[28]; ◇, Samimy and Elliott[29]; ∗, Sullins *et al.*[30]; +, Messersmith *et al.*[31]; ×, Chinzei *et al.*[32].

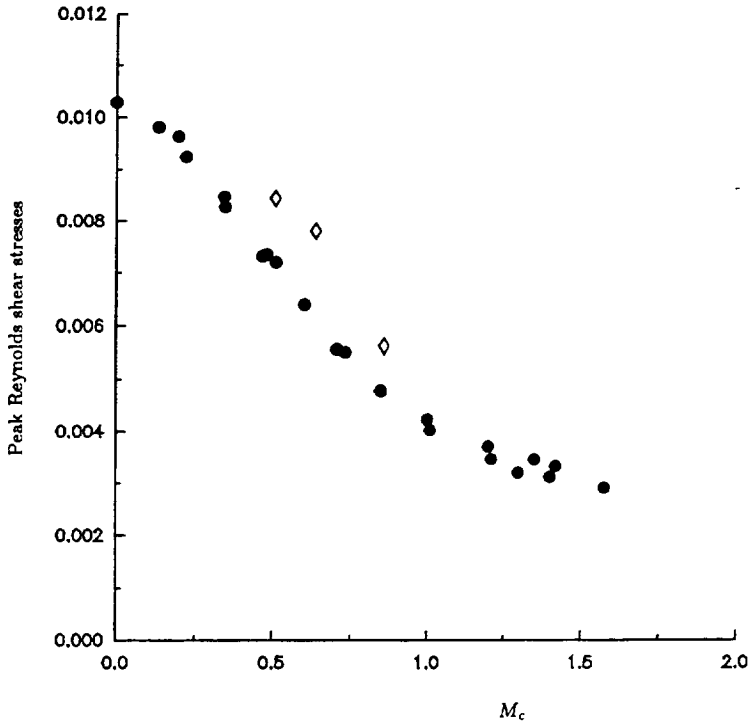

Figure 8. Variation of the peak Reynolds shear stress with convective Mach number. • , present model; ◇ , Elliott and Samimy[33].

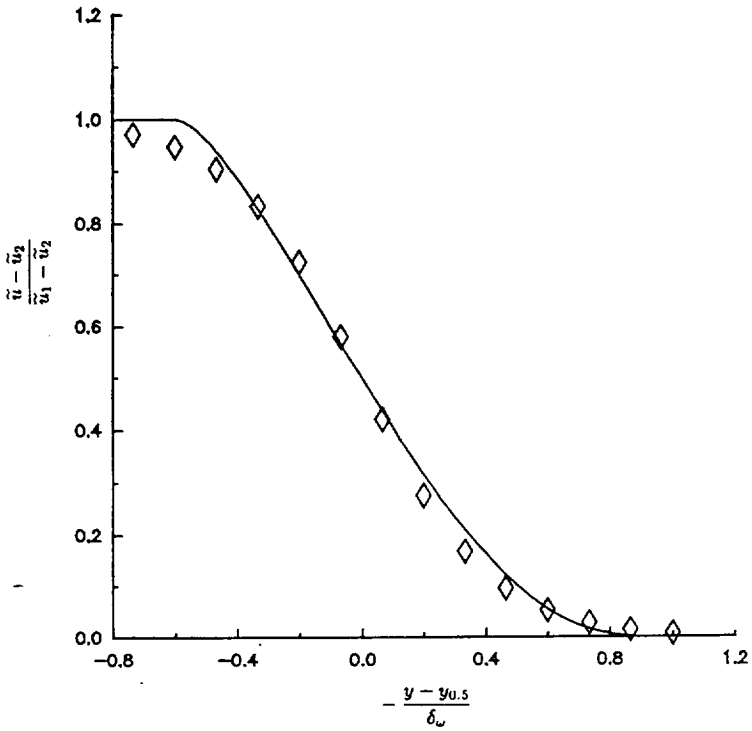

Figure 9. Nondimensional axial mean velocity profiles for the compressible shear layer of M_c = 0.51.——, present model; ◇ , case 1 of Elliott and Samimy[29].

REPORT DOCUMENTATION PAGE

Form Approved
OMB No. 0704-0188

1. AGENCY USE ONLY (Leave blank)	2. REPORT DATE	3. REPORT TYPE AND DATES COVERED
	March 1993	Technical Memorandum

4. TITLE AND SUBTITLE

A Multiple-Scale Model for Compressible Turbulent Flows

5. FUNDING NUMBERS

WU-505-90-5K

6. AUTHOR(S)

William W. Liou and Tsan-Hsing Shih

7. PERFORMING ORGANIZATION NAME(S) AND ADDRESS(ES)

National Aeronautics and Space Administration
Lewis Research Center
Cleveland, Ohio 44135-3191

8. PERFORMING ORGANIZATION REPORT NUMBER

E-7679

9. SPONSORING/MONITORING AGENCY NAMES(S) AND ADDRESS(ES)

National Aeronautics and Space Administration
Washington, D.C. 20546-0001

10. SPONSORING/MONITORING AGENCY REPORT NUMBER

NASA TM-106072
ICOMP-93-07
CMOTT-93-02

11. SUPPLEMENTARY NOTES

William W. Liou and Tsan-Hsing Shih Institute for Computational Mechanics in Propulsion and Center for Modeling of Turbulence and Transition, NASA Lewis Research Center, (work funded under NASA Cooperative Agreement NCC3-233). ICOMP Program Director, Louis A. Povinelli, (216) 433-5818.

12a. DISTRIBUTION/AVAILABILITY STATEMENT

Unclassified - Unlimited
Subject Category 34

12b. DISTRIBUTION CODE

13. ABSTRACT ***(Maximum 200 words)***

A multiple-scale model for compressible turbulent flows is proposed in this paper. It is assumed that turbulent eddy shocklets are formed primarily by the "collisions" of large energetic eddies. The extra straining of the large eddy, due to their interactions with shocklets, enhances the energy cascade to smaller eddies. Model transport equations are developed for the turbulent kinetic energies and the energy transfer rates of the different scale. The turbulent eddy viscosity is determined by the total turbulent kinetic energy and the rate of energy transfer from the large scale to the small scale, which is different from the energy dissipation rate. The model coefficients in the modeled turbulent transport equations depend on the ratio of the turbulent kinetic energy of the large scale to that of the small scale, which renders the model more adaptive to the characteristics of individual flow. The model is tested against compressible free shear layers. The results agree satisfactorily with measurements.

14. SUBJECT TERMS

Compressible flow; Turbulence modeling; Multiple-scale model

15. NUMBER OF PAGES

22

16. PRICE CODE

A03

17. SECURITY CLASSIFICATION OF REPORT	18. SECURITY CLASSIFICATION OF THIS PAGE	19. SECURITY CLASSIFICATION OF ABSTRACT	20. LIMITATION OF ABSTRACT
Unclassified	Unclassified	Unclassified	